MOLECULAR AND CELLULAR BIOLOGY, Sept. 2007, p. 6026–6037 Vol. 27, No. 17
0270-7306/07/$08.00+0 doi:10.1128/MCB.00384-07

Aquaporin 7 Is a β-Cell Protein and Regulator of Intraislet Glycerol Content and Glycerol Kinase Activity, β-Cell Mass, and Insulin Production and Secretion▽†

Kazuhiro Matsumura,[1,2]‡ Benny Hung-Junn Chang,[1]‡* Mineko Fujimiya,[3] Weiqin Chen,[1] Rohit N. Kulkarni,[4] Yutaka Eguchi,[5] Hiroshi Kimura,[2] Hideto Kojima,[1,2] and Lawrence Chan[1]*

Division of Diabetes, Endocrinology & Metabolism, Departments of Medicine and Molecular & Cellular Biology, Baylor College of Medicine, One Baylor Plaza, Houston, Texas 77030[1]; Department of Molecular Genetics in Medicine,[2] Department of Anatomy,[3] and Department of Critical and Intensive Care Medicine,[5] Shiga University of Medical Science, Otsu, Japan; and Joslin Diabetes Center, Harvard Medical School, Boston, Massachusetts 02215[4]

Received 2 March 2007/Returned for modification 24 April 2007/Accepted 5 June 2007

To investigate if intracellular glycerol content plays a role in the regulation of insulin secretion in pancreatic β cells, we studied the expression of the glycerol channels, or aquaglyceroporins, encoded by the aquaporin 3 (*Aqp3*), *Aqp7*, and *Aqp9* genes in mouse islets. We found expression of *Aqp7* only, not that of *Aqp3* or *Aqp9*, in the endocrine pancreas at both the mRNA (by reverse transcription-PCR) and protein (by immunohistochemistry) levels. Immunohistochemistry revealed a complete overlap between insulin and *Aqp7* immunostaining in the pancreatic islet. Inactivation of *Aqp7* by gene targeting produced viable and healthy mice. *Aqp7*$^{-/-}$ mice harbored an increased intraislet glycerol concentration with a concomitant increase of the glycerol kinase transcript level and enzyme activity. The islet triglyceride content in the *Aqp7*$^{-/-}$ mice was also increased compared to that in the *Aqp7*$^{+/+}$ mice. Interestingly, *Aqp7*$^{-/-}$ mice displayed reduced β-cell mass and insulin content but increased insulin-1 and insulin-2 mRNAs. The reduction of β-cell mass in *Aqp7*$^{-/-}$ mice can be explained at least in part by a reduction in cell proliferation through protein kinase C and the c-*myc* cascade, with a reduction in the transcript levels of these two genes. Concomitantly, there was a decreased rate of apoptosis, as reflected by terminal deoxynucleotidyltransferase-mediated dUTP-biotin nick end labeling and caspase 3 and Bax expression in *Aqp7*$^{-/-}$ mice. Compared with *Aqp7*$^{+/+}$ islets, islets isolated from *Aqp7*$^{-/-}$ mice secreted insulin at a higher rate under basal low-glucose conditions and on exposure to a high (450 mg/dl) glucose concentration. *Aqp7*$^{-/-}$ mice exhibited normal fasting blood glucose levels but elevated blood insulin levels. Their plasma glucose response to an intraperitoneal (i.p.) glucose tolerance test was normal, but their plasma insulin concentrations were higher than those of wild-type mice during the 2-h test. An i.p. insulin tolerance test showed similar plasma glucose lowering in *Aqp7*$^{-/-}$ and *Aqp7*$^{+/+}$ mice, with no evidence of insulin resistance. In conclusion, we found that pancreatic β cells express AQP7, which appears to be a key regulator of intraislet glycerol content as well as insulin production and secretion.

Glucose is the most important nutrient that regulates insulin secretion (21). In addition to its key role in insulin secretion, plasma glucose also regulates β-cell mass; in insulin-resistant states, the β-cell mass increases to provide sufficient insulin to keep the plasma glucose concentration in check. Therefore, glucose appears to play dual roles as a stimulus both for acute insulin secretion and for a compensatory increase in β-cell mass (8). Unlike glucose, glycerol, a triose sugar, has no apparent effect on insulin secretion (37, 39), though a closely related metabolite, glyceraldehyde, has a potent effect (1, 2). One reason that glycerol does not function as a signal for insulin secretion is that it appears not to be metabolized by pancreatic β cells (37). Induced overexpression of glycerol kinase (GYK) by adenovirus-mediated gene transfer in the rat insulinoma cell line INS-1 (37) or isolated rat pancreatic islets stimulates proinsulin biosynthesis (39) and insulin secretion (37, 39). Thus, the introduction of a glycerol-metabolizing enzyme to generate stimulus-response coupling signals downstream of glycerol metabolism enabled the exploration of the possible metabolic coupling signals involved in proinsulin biosynthesis and insulin secretion in vitro (37, 39).

To investigate if glycerol plays a key role in regulating β-cell function in vivo, we analyzed isolated pancreatic islets for the presence of glycerol channels. The known mammalian glycerol channels are members of the aquaporin (AQP) family, with 13 described members (3, 11) that fall into the following two major classes: (i) AQPs that function exclusively as water channels and (ii) AQPs that transport both water and glycerol or other small solutes, collectively known as aquaglyceroporins. Only four mammalian AQP sequences have been identified as potential aquaglyceroporins, namely, *Aqp3* (9, 18), *Aqp7* (31), *Aqp9* (5, 41), and *Aqp10* (17, 34). However, murine *Aqp10* was found to be a pseudogene (35). For this communication, we found that of the three functional aquaglyceroporins, only *Aqp7* is expressed in the β cells of pancreatic islets. To deduce

* Corresponding author. Mailing address: Division of Diabetes, Endocrinology & Metabolism, Departments of Medicine and Molecular & Cellular Biology, Baylor College of Medicine, One Baylor Plaza, Houston, TX 77030. Phone: (713) 798-4478. Fax: (713) 798-8764. E-mail for Benny Hung-Junn Chang: bchang@bcm.edu. E-mail for Lawrence Chan: lchan@bcm.edu.

† Supplemental material for this article may be found at http://mcb.asm.org/.

‡ K.M. and B.H.-J.C. contributed equally to this work.

▽ Published ahead of print on 18 June 2007.

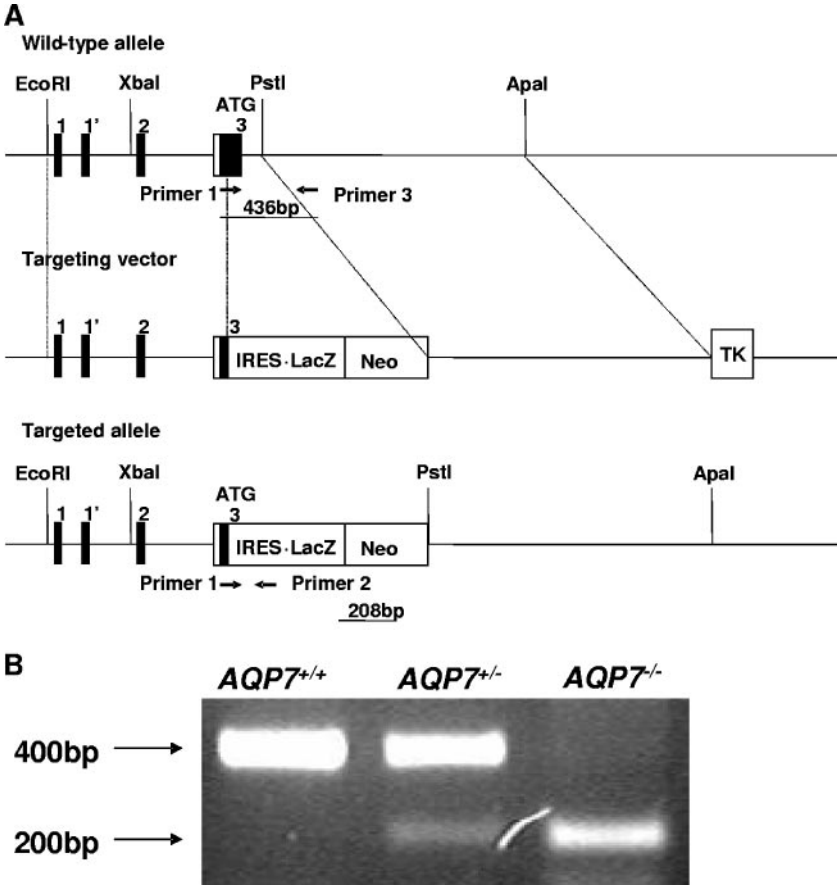

FIG. 1. Gene-targeting strategy for the inactivation of *Aqp7* in mice. (A) Restriction maps of the *Aqp7* gene (top), the targeting vector (middle), and the targeted recombinant allele (bottom) are shown. The locations of PCR primers 1, 2, and 3 used for genotyping are shown. (B) PCR screening of $Aqp7^{+/+}$, $Aqp7^{+/-}$, and $Aqp7^{-/-}$ mice. The PCR product for the wild-type allele is 430 bp, and that for the mutant allele is 208 bp.

the functional role of *Aqp7*, we produced mice with inactivated *Aqp7* by gene targeting. *Aqp7* knockout mice have been reported from three independent laboratories (13, 33, 40). While these reports support a role for *Aqp7* in adipose tissue and the kidneys, herein we document that *Aqp7* is expressed in the pancreatic islet and is important in the regulation of insulin production and secretion. We generated $Aqp7^{-/-}$ mice and found that they develop hyperinsulinemia in the absence of detectable insulin resistance. Furthermore, analysis of the pancreatic islets revealed that $Aqp7^{-/-}$ mice have an elevated intraislet glycerol concentration; they also display reduced β-cell mass and increased insulin mRNA but reduced intracellular insulin content. We conclude that *Aqp7* plays a key role in controlling β-cell mass and insulin production in vivo.

MATERIALS AND METHODS

Generation of *Aqp7* knockout mice. *Aqp7* genomic DNA was isolated from a 129/SV mouse genomic library. A replacement targeting construct containing a *PGK-NEO* cassette, an internal ribosome entry site (IRES)–β-galactosidase gene, and a herpes simplex virus thymidine kinase cassette was used as the targeting vector. The *PGK-NEO* cassette and IRES–β-galactosidase gene were inserted to replace a genomic region containing the second half of exon 3 and part of intron 4 of the mouse *Aqp7* gene (Fig. 1A). The linearized vector was electroporated into R1 embryonic stem (ES) cells (36), and after double selection with G418 and FIAU (1-[2′-deoxy-2′-fluoro-1-β-D-arabinofuranosyl]-5-iodouridine), knockout clones were generated as described previously (6). The ES cells carrying the correct mutation were injected into C57BL/6J blastocysts. Resulting male chimeras were mated to female C57BL/6J mice. Germ line transmission was confirmed by PCR, using tail DNA. Except for the growth curves for which we followed the mice for over 6 months, all experiments were performed on 14- to 18-week-old animals. All animal studies were conducted according to the *Principles of Laboratory Animal Care* (36a) and the guidelines of the IACUC of Baylor College of Medicine.

Gene expression analyses. We used TRIzol (Invitrogen, Carlsbad, CA) to isolate total RNA from tissues and cells. Reverse transcription was performed on 5 μg of RNA, using Superscript II (Invitrogen) according to the manufacturer's protocol. The expression of *Aqp3*, *Aqp7*, and *Aqp9* was detected by reverse transcriptase PCR (RT-PCR) using gene-specific primers in the following reaction thermoprofile: 94°C for 30 s, 56°C for 30 s, and 72°C for 60 s for 25 to 30 cycles. All PCR products were confirmed by direct sequencing. We performed quantitative real-time PCR with a LightCycler Fast Start DNA Master SYBR green I kit (Roche Diagnostics). The PCR mixture contained 20 ng of cDNA and the primers. Emitted fluorescence for each reaction was measured three times during the annealing/extension phase of each cycle, and amplification plots were analyzed by use of LightCycler software, version 3.4 (Roche Diagnostics). The relative value for each sample was calculated by a standard curve obtained with control samples (isolated islets from wild-type mice and B47 β cells) and standardized as the quotient of the sample value divided by the value simultaneously obtained with glyceraldehyde-3-phosphate dehydrogenase (GAPDH) in the same experiment. The mouse beta-actin gene was also used as a housekeeping gene control, which produced similar results to those with GAPDH. Data based on the latter are shown in this study.

The sequences of the primers are listed in Table 1.

Pancreatic islet isolation and culture. We isolated pancreatic islets from $Aqp7^{-/-}$ and wild-type mice as described previously (29). Following digestion and washing, mouse islets were handpicked under a stereomicroscope. We then

TABLE 1. Quantitative PCR primers used in this study

Gene	Primer sequence (5′ to 3′)	
	Forward	Reverse
Aqp3	ATGGGTCGACAGAAGGAGTTG	TCAGATCTGCTCCTTGTG
Aqp7	ATGGCCCCCAGGTCTGTGCTG	TTAGAAGTGCTCTAGAGGCACAGAGCC
Aqp9	ATGCCTTCTGAGAAGGACCG	CTACATGATGACGCTGAGTTCG
Pkc-β*2*	GCAGAAGAACGTGCACGAGG	CGTGACGAACTCATGGCAGC
c-*myc*	CAAATCCTGTACCTCGTCCG	GGTTTGCCTCTTCTCCACAG
Ins-1	GGAGCGTGGCTTCTTCTACA	GGTGGGCCTTAGTTGCAGTA
Ins-2	TCTACAATGCCACACTTCTG	TTTGTCAAGCAGCACCTTTG
Glucagon gene	ATGAAGACCATTTACTTTGTGGCTG	CGGCCTTTCACCAGCCACGC
Pancreatic polypeptide gene (*Pp*)	ATGGCCGTCGCATACTGCTG	TCGCTCCAGGGCGCAGAGC
Somatostatin gene	ATGCTGTCCTGCCGTCTCCA	CTAACAGGATGTGAATGTCTTCCAGAAGAA
Caspase 3 gene	CTCTGGTACGGATGTGGACG	CACACACACAAAGCTGCTCC
Bax	CCCTGTGCACTAAAGTGCCC	CTTCTTCACGATGGTGAGCG
Bcl-XL	CAGCAGTGAAGCAAGCGCTG	GATGCGACCCCAGTTTACTC
Bcl2	CTACGAGTGGGATGCTGGAG	GGTCAGATGGACACATGGTG
Gapdh	GTGTCTTCACCACCATGGAG	GTCATGGATGACCTTGGCC
Gyk	ATCCGCTGGCTAAGAGACAA	AGGCGCATATAACCCTGAAA
Beta-actin gene	GACGGCCAGGTCATCACTAT	CTTCTGCATCCTGTCAGCAA

cultured the islets at 37°C in a humidified atmosphere containing 5% CO_2. The culture medium was RPMI 1640 (11 mM glucose) supplemented with 10% fetal calf serum, 10 mM HEPES (pH 7.4), 1 mM sodium pyruvate, 2 mM glutamine, 100 IU/ml penicillin, and 100 μg/ml streptomycin (RPMI complete). All islet experiments were performed following 18 h of culture after isolation to allow recovery from the collagenase digestion and to optimize secretion in response to glucose.

We measured insulin in the medium by using Crystal Chem enzyme-linked immunosorbent assay kits (Chicago, IL). Isolated islets were collected in a cocktail with phosphate-buffered saline–Tween 20 and protease inhibitor from Roche (Indianapolis, IN), homogenized, and centrifuged at 3,000 × *g* for 15 min, and insulin and glycerol contents in the total lysate were measured using enzymatic kits (Sigma, St. Louis, MO).

For lipid extraction, 100 isolated islets were washed in cold PBS two times. We transferred islets into a capped glass tube with 3 ml chloroform-methanol (2:1) and stored them under N_2 at 4°C overnight. We added H_2O, vortexed the sample, centrifuged it at 1,076 × *g* for 10 min, carefully removed the lower layer into a new tube, and discarded the upper layer. The extraction was repeated two times. We dried the organic phase with N_2, stored the tube at −80°C, and then measured triglycerides by using enzymatic kits (Sigma, St. Louis, MO).

Cell culture experiments. We prepared β-cell lines by breeding wild-type mice with simian virus 40 T antigen (RIP-Tag2) transgenic mice driven by the insulin promoter as described previously (10, 29). Briefly, tumors from 10- to 12-week-old RIP-Tag2 mice were manually disrupted and placed in Dulbecco's modified Eagle medium supplemented with fetal calf serum. The tumor capsule was gently disrupted to release the cells, which were purified by gravity sedimentation, resuspended, seeded in 48-well plates, and allowed to attach. Individual clones that were responsive to glucose were picked for experiments. Experiments were performed with cells derived from a single clone (B47) obtained between passages 7 and 10.

B47 β cells were cultured in Dulbecco's modified Eagle medium containing 100 mg/dl of glucose, 10% fetal bovine serum, 100 units/ml penicillin, and 0.1 mg/ml streptomycin sulfate at 37°C in 5% CO_2 in air. After incubation with 0.1 μM of 12-o-tetradecanoylphorbol 13-acetate (TPA; Sigma), an activator of protein kinase C (PKC), with 100 μM of 1-(5-isoquinoline sulfonyl)-2-methylpiperazine (H7; Sigma Chemical Co.), an inhibitor of PKC, or with both TPA and H7 at 37°C for 6 h, we performed quantitative real-time RT-PCR using the RNAs isolated from these cells.

Immunohistochemical analysis. Pancreases, testes, kidneys, and livers from wild-type and $Aqp7^{-/-}$ mice were fixed and cut into 20-μm-thick sections in a cryostat. We incubated sections with antibody against AQP7 (goat polyclonal; Santa Cruz Biotechnology, CA), AQP3 (goat polyclonal; Santa Cruz Biotechnology, CA), or AQP9 (goat polyclonal; Santa Cruz Biotechnology, CA), diluted 1:2,000 in PBS containing 0.3% Triton X-100, at 4°C for 2 days (14, 27). Sections were then incubated for 2 h at room temperature with Alexa 488-labeled antibody against goat immunoglobulin G (IgG; Molecular Probes, Eugene, OR) diluted 1:1,000 in PBS–0.3% Triton X-100. For immunofluorescence overlap staining of AQP7 and islet hormones, pancreas sections were incubated with antibody against AQP7 (goat polyclonal) mixed with antibody against insulin (guinea pig polyclonal; Linco Research, St. Charles, MO), glucagon (rabbit polyclonal; Biogenesis, Kingston, NH), somatostatin (rabbit polyclonal; Yanaihara Ins., Shizuoka, Japan), or pancreatic polypeptide (rabbit polyclonal; Yanaihara Ins.). After reaction with the primary antibodies, sections were incubated with fluorescein isothiocyanate-labeled anti-goat IgG (Chemicon, Temecula, CA) mixed with either Cy3-labeled anti-guinea pig IgG (Chemicon) or Cy3-labeled anti-rabbit IgG (Chemicon). Sections were mounted on glass slides, dried, coverslipped with Histofine (Nichirei, Tokyo, Japan), and observed under a confocal laser scanning microscope (LSM 510; Carl Zeiss) as 1-μm slices (27).

Islet density. Pancreases from four $Aqp7^{+/+}$ and four $Aqp7^{-/-}$ mice were fixed and cut into 20-μm-thick serial sections in a cryostat. Five sections were randomly selected for each animal and processed for insulin immunohistochemistry using the ABC and nickel-DAB methods (27). The images of stained islets were transferred to a computer-assisted image analyzer (Luzex X-F; Nikon, Tokyo,

TABLE 2. Lipid, glucose, and insulin contents of plasmas and isolated islets from $Aqp7^{+/+}$ and $Aqp7^{-/-}$ mice ($n = 4$) fasted for 4 h[a]

Mouse group	Plasma level						Islet glycerol concn (μg/mg protein)	Pancreas triglyceride concn (μg/mg protein)	Islet insulin concn (ng/mg protein)
	Triglycerides (mg/dl)	Cholesterol (mg/dl)	Free fatty acids (mmol/liter)	Glycerol (mg/dl)	Glucose (mg/dl)	Insulin (pg/ml)			
Male mice									
$Aqp7^{+/+}$	26.4 ± 7.7	93.5 ± 16.7	0.71 ± 0.11	7.3 ± 1.6	144.8 ± 25.2	257.4 ± 160.3	11.9 ± 0.3	5.1 ± 0.4	95.1 ± 1.2
$Aqp7^{-/-}$	25.4 ± 5.8	86.8 ± 7.6	0.65 ± 0.07	7.5 ± 0.3	163.3 ± 7.6	1,207.0 ± 453.6*	25.9 ± 7.3*	13.9 ± 1.2*	71.9 ± 9.7*
Female mice									
$Aqp7^{+/+}$	36.5 ± 5.6	83.7 ± 16.4	0.85 ± 0.05	3.7 ± 0.6	140.8 ± 8.1	137.0 ± 29.9	16.7 ± 1.0	5.7 ± 0.6	131.6 ± 4.6
$Aqp7^{-/-}$	33.7 ± 3.1	72.9 ± 8.2	0.78 ± 0.13	3.4 ± 0.3	147.2 ± 18.8	519.2 ± 226.3*	36.9 ± 0.8*	15.7 ± 2.3*	106.9 ± 6.7*

[a] *, significant difference between $Aqp7^{+/+}$ and $Aqp7^{-/-}$ mice ($P < 0.05$).

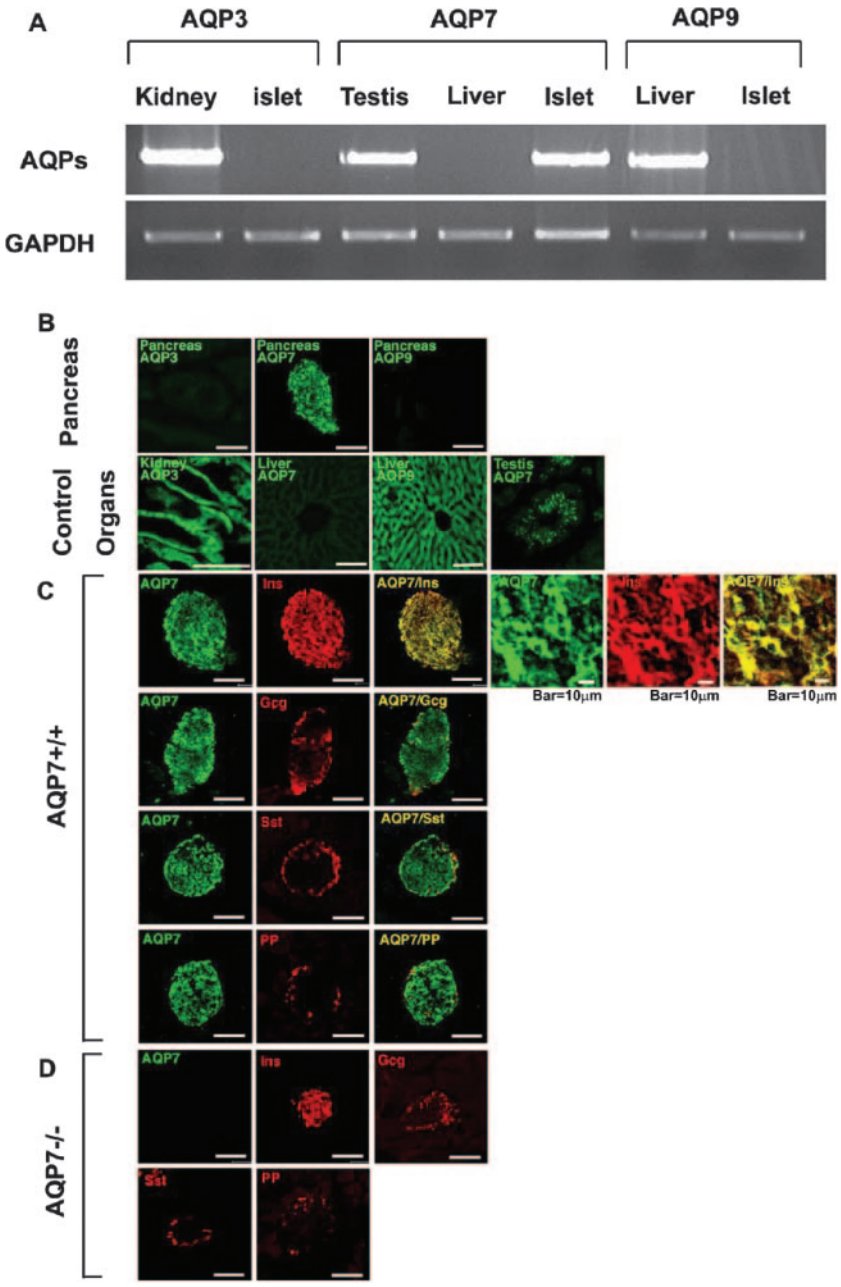

FIG. 2. AQP7 expression in mouse pancreatic islets. (A) RT-PCR analysis of three aquaglyceroporin genes, *Aqp3*, *Aqp7*, and *Aqp9*, in isolated islet, kidney, testis, and liver tissues from wild-type mice. *Gapdh* was used as an internal control. (B) Confocal laser microscopic analysis of the immunolocalization of AQP3, -7, and -9 in the pancreas, kidneys, liver, and testes (positive control of AQP7). (C and D) Confocal laser microscopic analysis of immunostaining images of AQP7 and 4 islet hormones in the pancreatic islets from wild-type ($Aqp7^{+/+}$) (C) and $Aqp7^{-/-}$ (D) mice. AQP7 expression completely overlaps with that of insulin (Ins) but not that of glucagon (Gcg), somatostatin (Sst), or pancreatic polypeptide (PP). Bars = 100 μm, unless marked otherwise.

Japan), and the total number and total area of islets were measured in each section. Area density (μm^2 of islets/mm^2 of pancreas) as well as islet density (number of islets/mm^2 of pancreas) was determined from five sections for each animal, and means ± standard deviations (SD) were obtained for four $Aqp7^{+/+}$ mice and four $Aqp7^{-/-}$ mice.

Densities of PCNA-positive and TUNEL-positive cells in pancreatic islets. Pancreases from wild-type mice and $Aqp7^{-/-}$ mice were fixed and cut into 20-μm-thick serial sections. We processed five randomly selected sections from each animal for PCNA immunohistochemistry as well as DeadEnd Colorimetric terminal deoxynucleotidyltransferase-mediated dUTP-biotin nick end labeling (TUNEL) analysis (Promega Corporation, Madison, WI). We counted the number of PCNA- or TUNEL-positive cells by light microscopy at a magnification of ×400, and the total islet area was obtained from an image analysis system as described above. The densities of PCNA-positive cells and of TUNEL-positive cells (number of positive cells/mm^2 of islet area) were estimated from five sections for each animal, and means ± SD were obtained for three wild-type mice and three $Aqp7^{-/-}$ mice.

Lipolysis in isolated islets. We isolated and washed batches of 100 islets in KRBH buffer (120 mM NaCl, 5 mM KCl, 2.5 mM $CaCl_2$, 1.1 mM $NaHCO_3$, 0.5% bovine serum albumin, and 10 mM HEPES, pH 7.4) and then incubated them for

2 h in 100 μl KRBH buffer containing 100 mg/dl glucose in a humidified incubator at 37°C. Once all islets were transferred, the same medium, with or without 2.5 μM forskolin, was added during the 2-hour incubation. At the end of the 2-h incubation, we collected the medium and measured the glycerol and Free fatty acid (FFA) released from islets by using enzymatic kits (Sigma, St. Louis, MO).

Metabolic experiments with isolated islets. For measurements of glucose usage, batches of 100 islets were washed in KRBH buffer and then incubated for 2 h in 100 μl KRBH buffer containing 40 mg/dl or 450 mg/dl glucose with 2.2 or 25 μCi/ml, respectively, of D-[5-^{3}H]glucose in a humidified incubator at 37°C. After removal of the supernatants, the islets were washed in KRBH buffer three times and then dissolved with 100 μl of 1 N NaOH. The samples were neutralized with 100 μl of 1 N HCl. Scintillation fluid was added to 100 μl of sample, and radioactivity was measured in a β-scintillation counter. The remaining 100 μl of each sample was used to measure protein content.

The experimental system for islet glucose oxidation assays consisted of a round-bottomed polystyrene 15-ml Falcon tube sealed with a rubber stopper from which a center well was suspended. Batches of 100 islets were washed in KRBH buffer and resuspended in 100 μl of KRBH buffer–0.5% bovine serum albumin (radioimmunoassay grade) containing 40 mg/dl or 450 mg/dl glucose with 3 or 16 μCi/ml, respectively, of [U-^{14}C]glucose. Islets in the glucose oxidation medium were then placed at the bottom of the Falcon tubes and sealed with the stoppers. After 3.5 h of incubation at 37°C in a cell incubator, the reaction was stopped with an injection of 0.1 ml perchloric acid (10% [vol/vol]). Benzethonium hydroxide (0.3 ml) was injected into the center well to trap the $^{14}CO_2$ produced. After an overnight incubation at room temperature, the benzethonium hydroxide was recovered, and scintillation fluid was added. Radioactivity was measured in a β-scintillation counter.

Determination of GYK activity. We performed a GYK activity assay as described previously (12), with a slight modification. Briefly, total pancreas or islets were homogenized in extraction buffer (50 mM HEPES, pH 7.8, 40 mM KCl, 11 mM $MgCl_2$, 1 mM dithiothreitol) on ice and centrifuged at 15,000 × *g* for 15 min at 4°C. Twenty to 30 μg of proteins was used for enzymatic assay. We incubated the protein samples with 50 μl of assay buffer (50 mM Tris-HCl, pH 7.2, 5 mM ATP, 10 mM $MgCl_2$, 100 mM KCl, 2.5 mM dithiothreitol, 4 mM glycerol, 50 μM [^{14}C]glycerol) for 3 h at 37°C. The reaction was terminated with 100 μl of stop solution (ethanol-methanol [97:3]). Equal amounts of the sample (50 μl) were spotted onto Whatman DE81 filters, and then the filters were air dried and washed in water overnight. Radioactivity adhering to the filters was measured by liquid scintillation.

Glucose tolerance test and insulin tolerance test. We injected a glucose solution (1.5 g/kg body weight intraperitoneally [i.p.]) into mice after a 4-h fast and obtained blood in EDTA 0, 15, 30, 60, and 120 min after glucose administration. Plasmas were separated and frozen at −20°C until glucose (Sigma kit) and insulin (Crystal Chem kit) determinations.

We injected insulin (1 U/kg body weight i.p.) into mice fasted for 4 h, obtained blood 0, 15, 30, 60, and 120 min afterwards, and measured plasma glucose and insulin as described above.

Statistical analysis. Results are expressed as means ± SD. The difference between *Aqp7*$^{+/+}$ and *Aqp7*$^{-/-}$ mice was evaluated by Student's *t* test. *P* values of <0.05 were taken as significant. Mann-Whitney nonparametric statistical analysis was done for experiments with small sample sizes ($n \leq 4$) to confirm the significance of differences.

RESULTS

Generation of *Aqp7*-inactivated mice. We used a gene replacement targeting strategy to inactivate the *Aqp7* gene in R1 mouse ES cells as shown in Fig. 1A. The mouse *Aqp7* gene contains a total of nine exons encoding two transcripts by using two alternative transcription initiation sites (exons 1 and 1′) (25). We used an IRES-LacZ-Neo cassette to replace a genomic region containing most of exon 3, where the translation initiation codon is located, and the neighboring intron of the *Aqp7* gene. Seven targeted ES cell clones were injected into blastocysts of C57BL/6J mice. PCR screening of tail DNAs from F1 mice revealed that the targeted locus had been transmitted to the progeny (Fig. 1B). Experiments performed on F3 and F4 *Aqp7*$^{-/-}$ mice and their wild-type littermate controls derived from two different ES clones produced similar results.

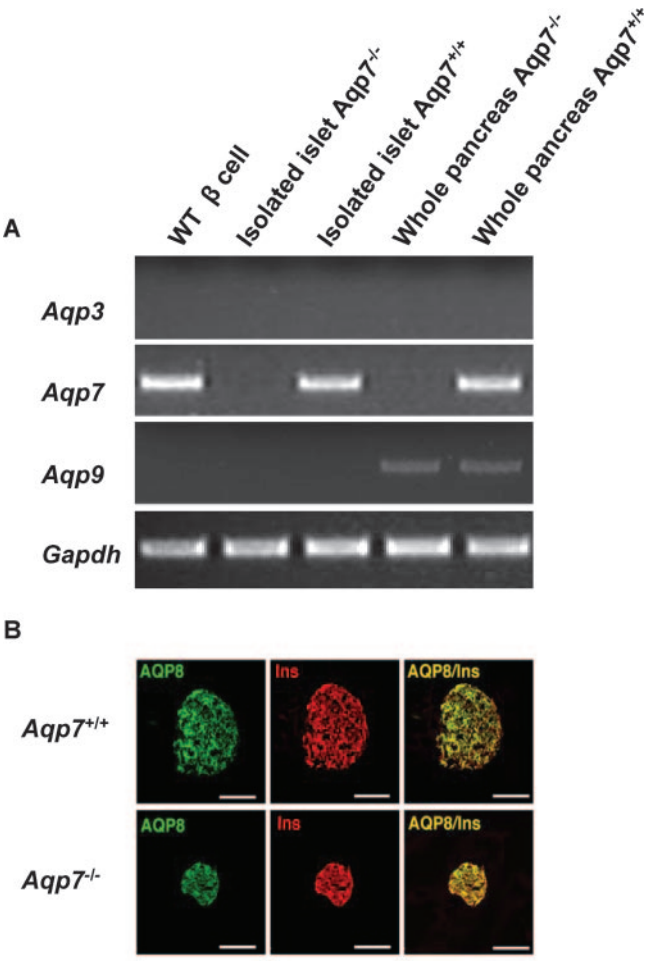

FIG. 3. *Aqp7* inactivation in *Aqp7*$^{-/-}$ tissues. (A) RT-PCR of *Aqp3*, *-7*, and *-9* transcripts, using RNAs isolated from the whole pancreas and isolated pancreatic islets from *Aqp7*$^{+/+}$ and *Aqp7*$^{-/-}$ mice and from WT β cell, a mouse β-cell line (B47). *Gapdh* was used as an internal control. (B) AQP8 is expressed in β cells of pancreatic islets.

Normal body weight and plasma chemistry in *Aqp7*$^{-/-}$ mice. Homozygous *Aqp7*$^{-/-}$ mice were viable and displayed normal body weights and growth curves as well as fat pad masses (see Fig. S1 in the supplemental material). *Aqp7*$^{-/-}$ mice did not show any abnormality in lipolysis (see Fig. S2 in the supplemental material) or in plasma lipid and plasma glucose contents (Table 2).

***Aqp7* is expressed in pancreatic islets.** *Aqp7* mRNA has been reported to be present in RNAs isolated from the whole pancreas of the rat (26). We confirmed the expression of *Aqp7* transcripts in mouse pancreas by RT-PCR and determined the cellular origin of the transcripts by analyzing RNAs extracted from isolated pancreatic islets. By RT-PCR, mouse islet RNAs contained only *Aqp7* mRNA, not *Aqp3* or *Aqp9* mRNA (Fig. 2A).

The pancreatic islet origin of AQP7 expression was confirmed at the protein level by immunohistochemistry. We localized AQP7 expression in pancreatic islets but not in pancreatic ducts or the acinar pancreas by this technique. The endocrine pancreas did not contain any detectable immunore-

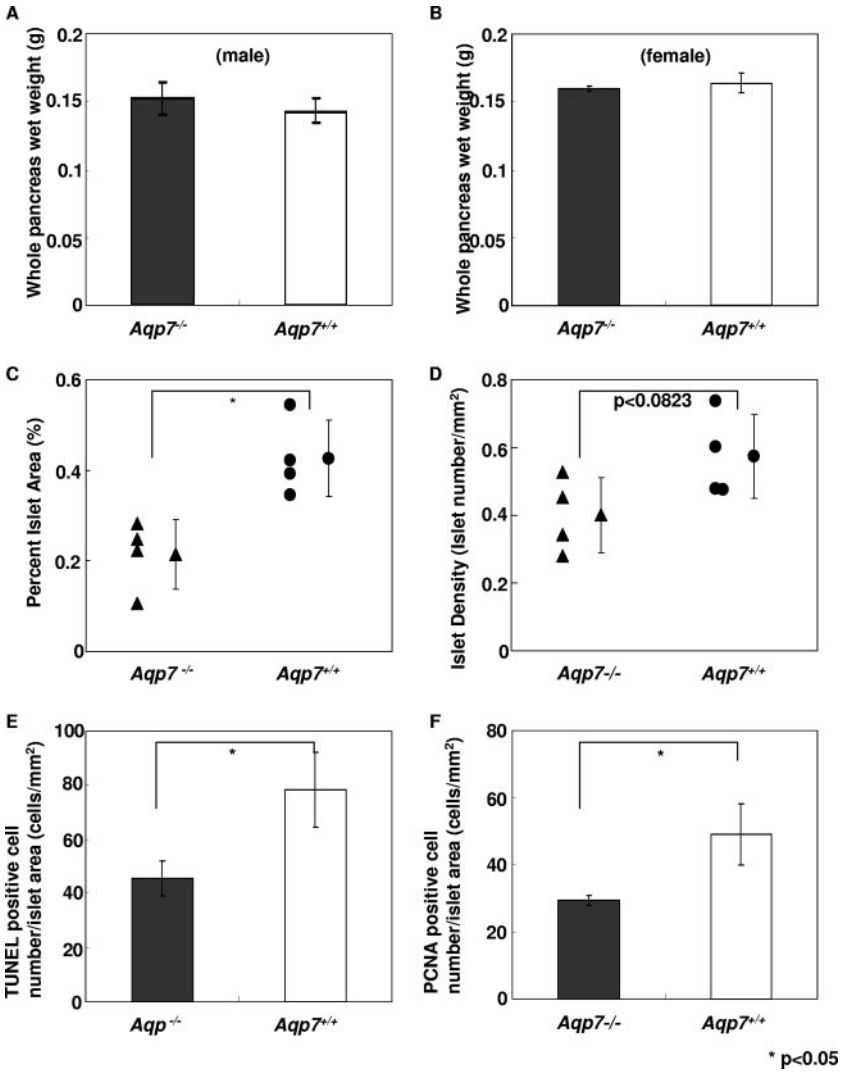

FIG. 4. Pancreas and pancreatic islet masses in $Aqp7^{-/-}$ mice and $Aqp7^{+/+}$ mice. (A and B) Whole pancreas wet weights for males (A) and females (B). Values are means ± SD ($n = 4$). (C) Total islet area. (D) Number of islets in whole pancreas ($n = 4$). (E and F) Density distributions of TUNEL (E)- and PCNA (F)-positive cells in islets. Values are means ± SD (data are for five sections from each of three animals).

active AQP3 or AQP9. To confirm the tissue specificity of immunostaining, we examined control tissues and found positive staining for AQP3 in the kidney and for AQP9 in the liver and the absence of AQP7 staining in the livers of wild-type mice (Fig. 2B).

Complete abrogation of *Aqp7* expression without compensatory upregulation of other aquaglyceroporins in $Aqp7^{-/-}$ islets. By RT-PCR, $Aqp7^{-/-}$ mice contained no detectable *Aqp7* transcripts in the pancreas or islets (Fig. 3A). *Aqp7* gene disruption did not affect the expression level of *Aqp3* and *Aqp9* in the total pancreas or islets (Fig. 3A). The disruption of *Aqp7* did not affect the normal expression of the water channel protein AQP8 in the islets (Fig. 3B).

***Aqp7* inactivation reduces islet size and total islet cell mass.** We used immunohistochemistry to localize AQP7 and the other major islet hormones in the pancreases of wild-type mice by confocal laser scanning microscopy and detected immunoreactive AQP7 in insulin-producing cells but not in glucagon-, somatostatin-, or pancreatic polypeptide-producing cells (Fig. 2C). *Aqp7* gene disruption completely abrogated *Aqp7* immunostaining in the pancreas. Insulin-producing cells were present in the pancreas in $Aqp7^{-/-}$ mice (Fig. 2D), but the insulin-positive cell clusters were smaller and not as well stained, suggesting that the intraislet insulin content was reduced (see below). There was also a persistence of glucagon-, somatostatin-, and pancreatic polypeptide-producing cells in $Aqp7^{-/-}$ islets (Fig. 2D). Whole pancreas weights were similar for $Aqp7^{-/-}$ mice and wild-type littermate controls (Fig. 4A and B). *Aqp7* inactivation reduced the mean insulin-immunoreactive area per islet cluster to about half that of controls (Fig. 4C). The reduction in the number of islet hormone-producing cells in $Aqp7^{-/-}$ islets also occurred with glucagon (87.9 ± 10.4 $\mu m^2/mm^2$ versus 181.7 ± 18.4 $\mu m^2/mm^2$ in wild-type islets; $P < 0.01$) and pancreatic polypeptide (22.2 ± 2.7 $\mu m^2/mm^2$ versus 50.3 ± 5.08 $\mu m^2/mm^2$ for wild-type islets; $P < 0.01$) but not with somatostatin (102.9 ± 12.2 $\mu m^2/mm^2$ versus 15.5 ± 6.4

TABLE 3. Relative gene expression levels quantified by quantitative RT-PCR using RNAs isolated from islets of *Aqp7*$^{-/-}$ mice compared to those from *Aqp7*$^{+/+}$ mice ($n = 3$)[a]

Gene	Relative expression ratio	*P* value (*t* test)[b]
PKCβ2 gene	0.23 ± 0.20	<0.05
c-*myc*	0.38 ± 0.04	<0.01
Ins-1	4.72 ± 0.24	<0.01
Ins-2	2.36 ± 0.34	<0.05
Glucagon gene	1.22 ± 0.33	NS
Somatostatin gene	1.10 ± 0.22	NS
Pancreatic peptide gene	0.72 ± 0.22	NS
Bax	0.38 ± 0.11	<0.01
Bcl2	0.35 ± 0.07	<0.01
Bcl-XL	0.13 ± 0.05	<0.01
Caspase 3	0.36 ± 0.18	<0.01
Aqp8	0.90 ± 0.35	NS
Glut2	10.51 ± 3.81	<0.05
Glucokinase gene	15.41 ± 5.59	<0.05
Glycerol kinase gene	6.55 ± 4.27	<0.004

[a] The GAPDH gene was used as the housekeeping control. The beta-actin gene was also used to reconfirm the results (not shown).
[b] NS, not significant.

$\mu m^2/mm^2$ for wild-type islets; $P = 0.191$). The number of islets per unit area (islet density) was unchanged statistically, but there was a trend towards fewer islets per unit area (Fig. 4D). Therefore, the total number of islets as well as the β-cell mass is reduced in *Aqp7*$^{-/-}$ mice. To determine if increased apoptosis might have contributed to the reduced islet cell mass, we determined the density of TUNEL-positive cells in the pancreatic islets. The number of TUNEL-positive cells was reduced in the islets of *Aqp7*$^{-/-}$ mice (Fig. 4E), ruling out increased apoptosis as a mechanism for the reduced islet mass. We next examined the density distribution of PCNA-positive cells, a measure of cell proliferation, and found that the absence of *Aqp7* was associated with a significant reduction in PCNA-positive cell staining (Fig. 4F). Therefore, reduced cellular proliferation contributed to the reduced islet mass in *Aqp7*$^{-/-}$ mice.

Proliferation- and apoptosis-related gene expression in islets of *Aqp7*$^{-/-}$ mice. To further explore the mechanism behind the reduced islet cell mass in *Aqp7*$^{-/-}$ mice, we analyzed the mRNA expression of several cell growth- and apoptosis-related genes. c-myc was found to stimulate islet cell proliferation following partial pancreatectomy (4, 20, 42) and glucose infusion-induced hyperglycemia (23, 24). We quantified c-*myc* mRNA expression by RT-PCR and found that it was suppressed in the islets of *Aqp7*$^{-/-}$ mice (Table 3). Since c-*myc* expression is regulated by PKC-β2 in pancreatic islets (24), we examined PKC-β2 mRNA expression by RT-PCR (Table 3) and found it to be reduced in the pancreatic islets of *Aqp7*$^{-/-}$ mice compared with that in *Aqp7*$^{+/+}$ controls. Western blotting indicated that the PKC-β2 protein was also downregulated in the islets (data not shown). To determine the role of *Aqp7* in c-*myc* regulation by PKC, we examined the effect of TPA, an activator of PKC, on B47 mouse β cells. We found that TPA

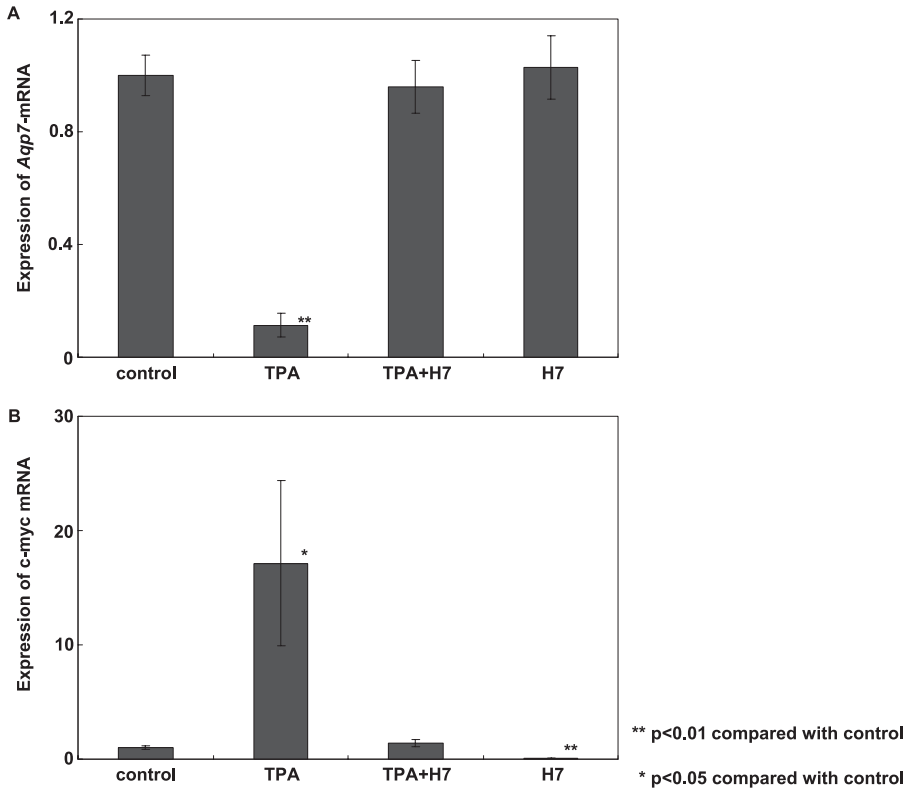

FIG. 5. Regulation of *Aqp7* and c-*myc* mRNA expression by PKC activator TPA and its inhibitor, H7, in β-cell line B47. Quantitative RT-PCR was performed for *Aqp7* (A) and c-*myc* (B) mRNA expression in B47 β cells in response to 6 h of treatment with 0.1 μM of TPA, 100 μM of H7, or both. Values shown are means ± SD ($n = 3$). **, $P < 0.01$; *, $P < 0.05$.

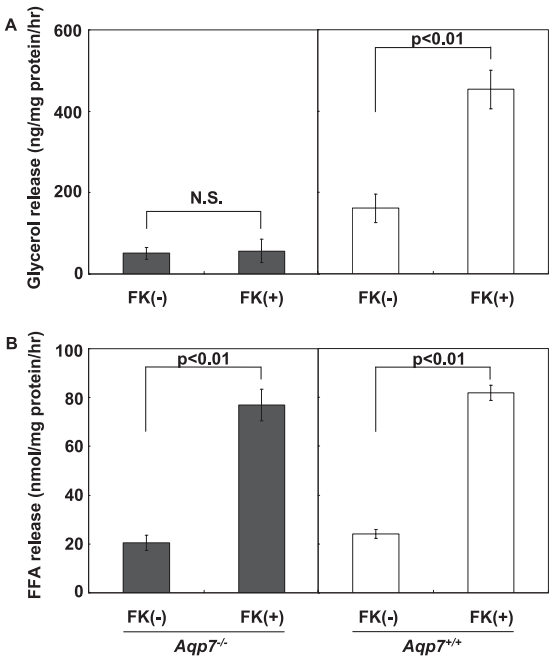

FIG. 6. Rate of lipolysis in isolated islets ($n = 3$). Batches of 100 islets were isolated from $Aqp7^{-/-}$ and $Aqp7^{+/+}$ mice and washed in KRBH buffer, and glycerol (A) and free fatty acid (B) release from these islets over a period of 2 h under basal or forskolin (FK; 2.5 μM)-stimulated conditions was determined using enzymatic kits.

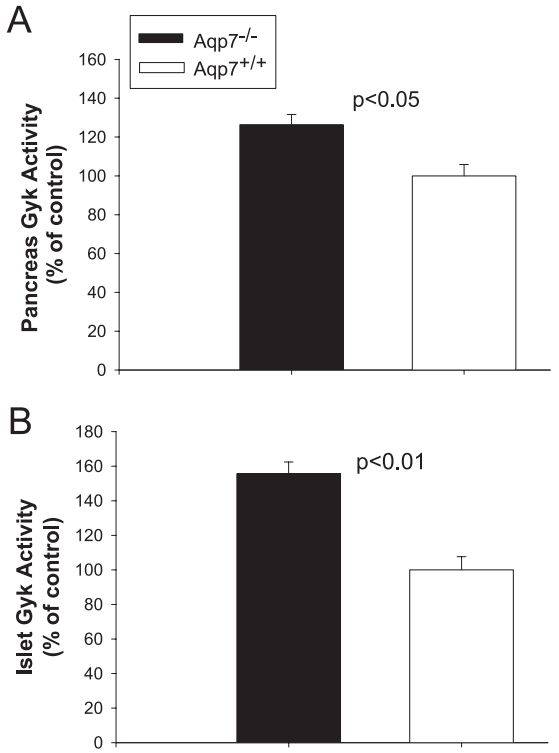

FIG. 7. GYK activity in pancreases from $Aqp7^{-/-}$ and $Aqp7^{+/+}$ mice. GYK enzyme activity (detailed in Materials and Methods) was measured using protein extracts from total pancreas (A; $n = 4$) or isolated islets (B; $n = 6$) of $Aqp7^{-/-}$ and $Aqp7^{+/+}$ mice that were fasted for 18 h. The data are percentages of the control value.

suppressed the expression of *Aqp7* and stimulated c-*myc* mRNA expression in these cells (Fig. 5A and B). This effect of TPA was completely abrogated by the addition of H7, a PKC inhibitor, which by itself inhibited c-*myc* expression.

Upregulation of c-*myc* was previously shown to suppress insulin gene transcription by inhibiting NeuroD/BETA2-mediated transcriptional activation (24). We investigated if c-*myc* downregulation in the islets of $Aqp7^{-/-}$ mice affects insulin gene expression. By RT-PCR, we found that $Aqp7^{-/-}$ islets contained increased amounts of insulin-1 and insulin-2 transcripts, indicating that the low c-*myc* expression was associated with enhanced insulin mRNA expression. There was no significant difference in the levels of transcripts for glucagon, somatostatin, and pancreatic polypeptide between $Aqp7^{-/-}$ and $Aqp7^{+/+}$ islets (Table 3).

To further document the effects of the absence of *Aqp7* on apoptosis-related genes, we examined the mRNA expression of some of the proapoptotic (caspase 3 and Bax) and antiapoptotic (Bcl2 and Bcl-XL) genes by RT-PCR (19). We found that the transcript levels for all four genes were reduced in the islets of $Aqp7^{-/-}$ mice (Table 3). The overall effect of the absence of *Aqp7* was a reduction in TUNEL positivity in the pancreatic islets. The reduction in caspase 3 and Bax is consistent with this effect and also with the known stimulatory effect of c-*myc* overexpression (7, 30). The simultaneous fall in the levels of Bcl2 and Bcl-XL, the antiapoptotic transcripts, could be a compensatory change in response to the reduction in apoptotic gene expression.

Increased glycerol content and reduced insulin content of islets of $Aqp7^{-/-}$ mice. AQP7 is a glycerol channel that allows the transport of glycerol from the inside of the cell to the outside (16). Consistent with a similar role for AQP7 in pancreatic β cells, we found that the absence of AQP7 was associated with a moderate increase in the glycerol content of the total pancreas, although β cells make up only 2% of the pancreas (data not shown); furthermore, we observed a >2-fold increase in the glycerol content of pancreatic islets isolated from $Aqp7^{-/-}$ mice compared with those isolated from $Aqp7^{+/+}$ mice (Table 2). Isolated $Aqp7^{-/-}$ islets secreted FFA under basal and forskolin-stimulated conditions (Fig. 6B). Forskolin treatment increased the intracellular cyclic AMP level and initiated PKA-mediated signaling events leading to the activation of hormone-sensitive lipase and increased lipolysis. The normal response of FFA release from $Aqp7^{-/-}$ islets suggested that lipolysis was intact compared to that in wild-type islets. However, under basal conditions, the release of glycerol was markedly reduced in $Aqp7^{-/-}$ islets compared to that in the wild-type islets; furthermore, forskolin-stimulated glycerol release observed in wild-type islets was completely abolished in $Aqp7^{-/-}$ islets (Fig. 6B). These data further support the role of AQP7 as a glycerol channel controlling glycerol export in pancreatic islets. Interestingly, the insulin content of $Aqp7^{-/-}$ islets was significantly reduced (Table 2), despite the presence of an increased intraislet insulin mRNA level (Table 3). This finding suggests that the insulin produced is secreted at an elevated rate from β cells of $Aqp7^{-/-}$ mice compared to that for cells of $Aqp7^{+/+}$ controls (see below).

Increased GYK activity of pancreases from $Aqp7^{-/-}$ mice. Using primary adipocytes, Hibuse et al. showed that *Aqp7* deficiency caused an activation of GYK resulting in an increase of the triglyceride content compared to that in wild-type adipocytes (15).

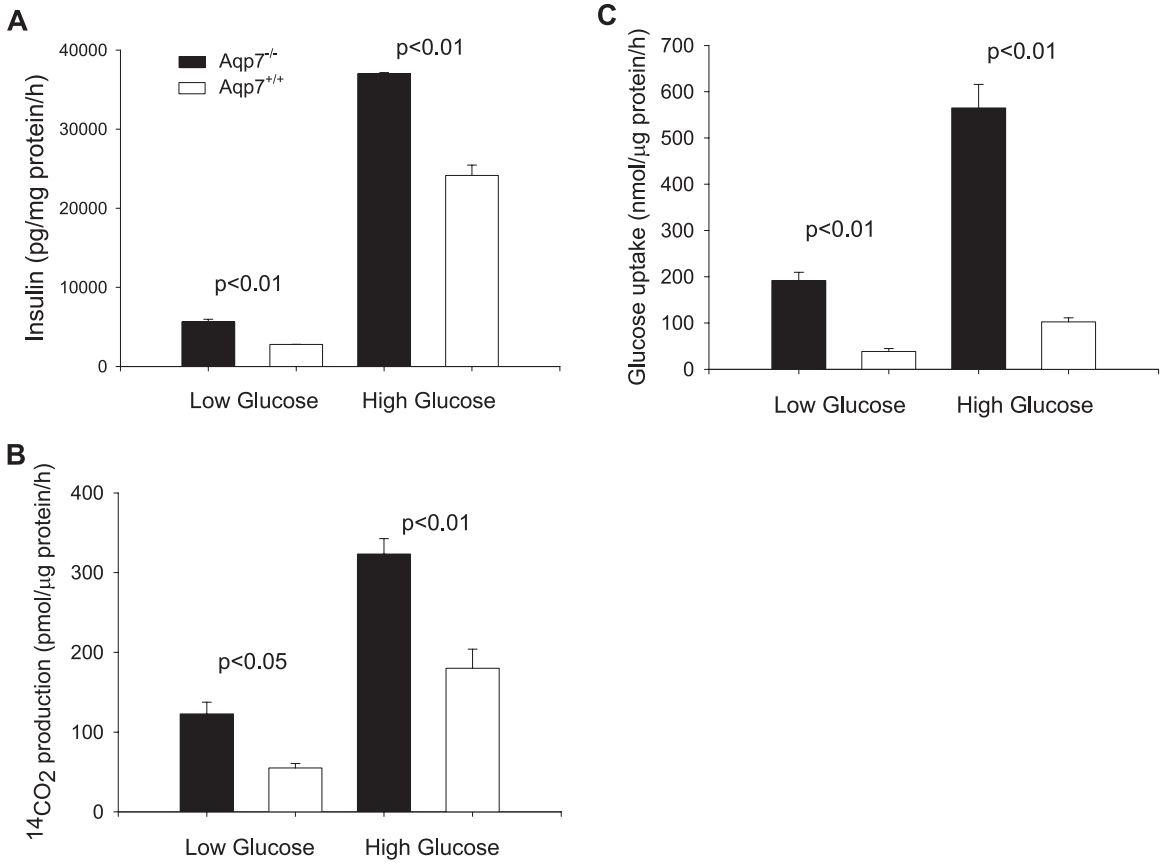

FIG. 8. Metabolism of islets isolated from *Aqp7*$^{-/-}$ and *Aqp7*$^{+/+}$ mice. Insulin secretion (A), CO_2 production (B), and glucose uptake (C) were measured from isolated islets incubated in low (100 mg/dl)- or high (450 mg/dl)-glucose medium. Black bars, islets from *Aqp7*$^{-/-}$ mice; white bars, islets from *Aqp7*$^{+/+}$ mice. Values are means ± SD (n = 3).

We measured *Gyk* mRNA expression by quantitative RT-PCR, using isolated islets from *Aqp7*$^{+/+}$ and *Aqp7*$^{-/-}$ mice. The *Gyk* mRNA level in the *Aqp7*$^{-/-}$ islets was 655% that in *Aqp7*$^{+/+}$ islets (Table 3). To determine if the increase in mRNA was reflected in an increase in GYK activity, we measured the GYK enzyme activity in total cell homogenates from the pancreas (Fig. 7A) and from isolated pancreatic islets (Fig. 7B). GYK activity was increased in both total pancreases (Fig. 7A) and islets (Fig. 7B) isolated from *Aqp7*$^{-/-}$ mice compared with those isolated from *Aqp7*$^{+/+}$ mice.

Islets of *Aqp7*$^{-/-}$ mice display increased insulin secretion, glucose uptake, and CO_2 production with a concomitant increase of *Glut2* and glucokinase gene transcription. We isolated pancreatic islets from mice of the two genotypes and measured their insulin secretion, glucose uptake, and CO_2 production when they were exposed to low-glucose and then elevated-glucose media. Compared with islets from *Aqp7*$^{+/+}$ mice, islets from *Aqp7*$^{-/-}$ mice displayed increased basal insulin secretion in low-glucose medium; they also showed a greater increase in the amount of insulin secreted in response to an elevated glucose concentration (Fig. 8A). CO_2 production and glucose uptake by islets isolated from *Aqp7*$^{-/-}$ mice were elevated compared to those by islets isolated from *Aqp7*$^{+/+}$ mice, both under basal conditions (low glucose) and under high-glucose stimulation (Fig. 8B and C).

We measured the levels of two different gene transcripts that regulate glucose-stimulated insulin secretion, namely, *Glut2*, the islet glucose transporter gene, and the gene for glucokinase (*Gk*), a rate-limiting enzyme in glucose-stimulated insulin secretion. The expression of these two genes was increased >10-fold in the islets of *Aqp7*$^{-/-}$ mice compared to that in the islets of the *Aqp7*$^{+/+}$ mice (Table 3).

Hyperinsulinemia in the absence of peripheral insulin resistance in *Aqp7*$^{-/-}$ mice. The increased insulin secretion from the isolated pancreatic islets of *Aqp7*$^{-/-}$ mice was associated with an elevated fasting plasma insulin level but a normal fasting plasma glucose concentration in *Aqp7*$^{-/-}$ mice compared to wild-type mice (Fig. 9A and B). Furthermore, *Aqp7*$^{-/-}$ mice had a normal plasma glucose response to an i.p. glucose tolerance test, accompanied by a persistent hyperinsulinemia throughout the 2-h test. An i.p. insulin tolerance test revealed a plasma glucose response that was not different from that of *Aqp7*$^{+/+}$ controls, indicating the absence of any detectable insulin resistance in these animals (Fig. 9C).

DISCUSSION

Aqp7-targeted mice have been produced independently by four different laboratories, including our laboratory; these mice show various degrees of difference in their phenotypic

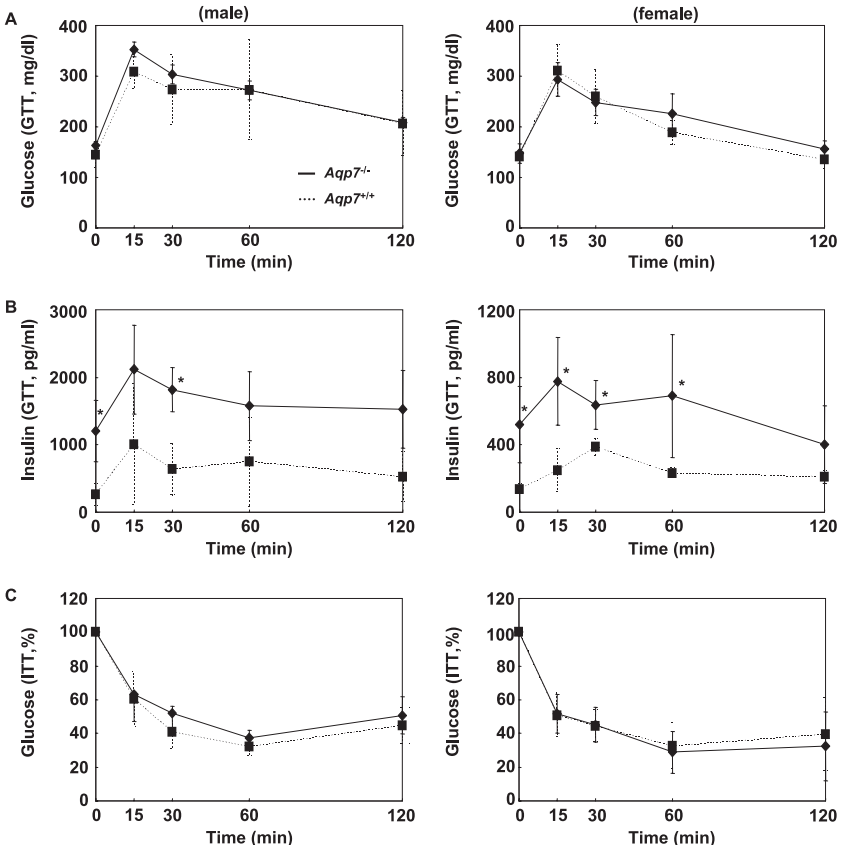

FIG. 9. Results of i.p. glucose tolerance (GTT) and insulin tolerance (ITT) tests. *Aqp7*$^{-/-}$ and *Aqp7*$^{+/+}$ mice ($n = 4$) were injected (i.p.) with 1.5 g/kg of body weight of glucose, and plasma glucose (A) and insulin (B) were measured at various times. Similarly, insulin was injected (i.p.) into *Aqp7*$^{-/-}$ and *Aqp7*$^{+/+}$ mice ($n = 4$) at 1 U/kg body weight, and plasma glucose (C) was measured at various times. ◆, *Aqp7*$^{-/-}$ mice; ■, *Aqp7*$^{+/+}$ mice. Values are means ± SD ($n = 4$). *, $P < 0.05$.

manifestations. Two earlier studies showed the importance of AQP7 in regulating glycerol transport in adipose tissues, with its absence resulting in a significant reduction of plasma glycerol and in increases of adipocyte cell volume and adipose tissue mass (13, 33). Increased body weight and derangement of whole-body metabolism were also observed in the aged *Aqp7*$^{-/-}$ mice in one of the studies (15). In contrast to these earlier studies, the *Aqp7*$^{-/-}$ mice that we generated, like those generated by Skowronski et al. (40), do not display any detectable difference in adipose size or volume. We also failed to detect any difference in body weights between wild-type and *Aqp7*$^{-/-}$ mice when we monitored them for 6 months (see Fig. S1 in the supplemental material). We detected no difference between *Aqp7*$^{+/+}$ and *Aqp7*$^{-/-}$ mice with respect to body weight, plasma lipids, and plasma glucose (see Table S1 in the supplemental material) as they aged (43 to 46 weeks); however, *Aqp7*$^{-/-}$ mice consistently showed higher plasma insulin levels than did *Aqp7*$^{+/+}$ mice. The mice generated by Skowronski et al. (40), however, lost large amounts of glycerol in the urine. It is likely that differences in mouse genetic backgrounds contributed to the observed differences in phenotypic manifestations. The models that showed adipose phenotypes were in the C57BL/6N and CD1 genetic backgrounds (13, 15), while the models generated by Skowronski et al. (40) and by us were in the predominantly C57 (mixed with 129) genetic background.

Experiments using adenovirus-mediated gene transfer of *Gyk* to an insulinoma cell line and isolated β cells showed that when glycerol is metabolized, it has the potential to stimulate proinsulin biosynthesis and insulin secretion (37, 39). In this study, we showed that an outward glycerol transport channel, AQP7, is expressed in β cells and that its inactivation causes glycerol to accumulate in the islets of *Aqp7*$^{-/-}$ mice, with a concomitant increase in *Gyk* mRNA expression and enzyme activity. The elevated intracellular glycerol level and GYK activity, in turn, stimulate proinsulin mRNA and insulin secretion, probably through their participation in glycolysis and glycerol-phosphate shuttle activities in the β cell (39). Interestingly, the increased insulin secretion in *Aqp7*$^{-/-}$ mice is accompanied by a reduction in the total β-cell mass (Fig. 5C and D), indicating a greatly increased efficiency in the insulin production/secretion process in these cells. These experiments provide direct evidence for the first time for the existence of an aquaglyceroporin in β cells; modulation of glycerol transport via AQP7 appears to be a mechanism by which proinsulin biosynthesis and insulin secretion are regulated in vivo (see below for further discussion). We further showed that in a mouse β-cell line, there is a reciprocal relationship between

c-*myc* and *Aqp7* expression. Stimulation of c-*myc* is associated with downregulation and suppression of c-*myc* is associated with upregulation of *Aqp7* (Table 3). The greatly reduced level of c-*myc* transcripts in $Aqp7^{-/-}$ islets (Table 3) suggests a feedback loop that coordinately controls the expression of these two proteins.

The islets of $Aqp7^{-/-}$ mice not only displayed increased insulin production and secretion but also had increased glucose uptake and oxidation under both basal and high-glucose conditions compared with $Aqp7^{+/+}$ mice. The elevated glucose uptake and utilization in $Aqp7^{-/-}$ islets can be explained by the upregulation of *Glut2* and *Gk* gene transcripts, although the exact mechanism needs to be studied in greater detail in the future. The result of increased glucose uptake and utilization may be an increase in the ratio of ATP to ADP, which further boosts insulin production and secretion. It is also possible that the islets of $Aqp7^{-/-}$ mice preferentially utilize glucose for energy production while the retained glycerol resulting from *Aqp7* deficiency is recycled to form triglycerides.

It is interesting that the $Aqp7^{-/-}$ mice developed hyperinsulinemia without manifest hypoglycemia. Hyperinsulinemia was also observed in the $Aqp7^{-/-}$ mice reported by Hibuse et al. (15), but it was accompanied by hyperglycemia, a sign of insulin resistance. Indeed, both glucose and insulin tolerance tests revealed abnormality in the $Aqp7^{-/-}$ mice they generated, with diminished insulin signaling in adipose, liver, and muscle tissues when they were treated with insulin. However, glucose and insulin tolerance tests showed normal responses in our $Aqp7^{-/-}$ mice, and there was no hyperglycemia in these animals. Of the *Aqp7*-inactivated mice reported from three other laboratories, insulin resistance was found in one (15) but was either not present or not studied by the other two laboratories (13, 40). Since *Aqp7* is expressed in multiple other insulin-responsive tissues, such as fat and muscle, complex compensatory tissue responses and/or the relative importance of this gene in mice of different genetic backgrounds may underlie the subtle differences in glucose homeostasis in animals generated from different laboratories.

It is generally believed that rat islet β cells or β-cell lines derived from rat islets do not express *Gyk* (37). However, we readily detected *Gyk* mRNA expression and protein activity in isolated mouse islets. Although the mouse and rat are closely related species, they differ in many of their insulin dynamics. For example, the islet insulin secretory response to glucose is different between mice and rats (43), with rats showing a much larger second-phase response to glucose stimulation. Furthermore, mice do not express malic enzyme in the islet, while rats do, and hence methyl succinate cannot induce insulin secretion in mouse islets (32), though it does so in rats. It is interesting that although *Gyk* had previously been thought to be absent in adipose tissue of mice, it is now known to be expressed there (12); thus, it is not surprising that *Gyk* is also expressed in mouse pancreatic islets. *Gyk* mRNA and enzyme activity were both increased in $Aqp7^{-/-}$ islets compared to those in wild-type islets. These increases were accompanied by a concomitant increase in triglyceride concentration in the islets of $Aqp7^{-/-}$ mice (Table 2). These observations are analogous to those of Hibuse et al., who found increased *Gyk* activity in the fat of $Aqp7^{-/-}$ mice (15). We surmise that parallel molecular mechanisms regulate *Gyk* expression in the two tissues.

Diabetes happens when there is inadequate insulin production in response to the body's demand for the hormone. Absolute insulin deficiency occurs in type 1 diabetes when β cells are destroyed by autoimmunity. In insulin-resistant states, such as obesity and type 2 diabetes, expansion of the β-cell mass occurs in response to the increased demand, but diabetes does not occur unless there is concomitant β-cell dysfunction (22). AQP7, which controls the cellular glycerol content, appears to play a key role in regulating proinsulin biosynthesis and insulin secretion. Recently, a single-nucleotide polymorphism was found in the promoter region of the human *AQP7* gene (38). This A-953G polymorphism was shown to reduce C/EBP-β DNA binding, resulting in the reduction of *AQP7* expression in a reporter assay system. This 953G variant is associated with diminished *AQP7* expression in the adipose tissues of obese individuals. The same variant is also associated with an increased risk of type 2 diabetes in human females. Unfortunately, the plasma insulin levels for different genotypes were only partially presented, and it is difficult to ascertain whether this *AQP7* variant contributes to hyperinsulinemia in humans like that we observed in the $Aqp7^{-/-}$ mice. An earlier case report described a human subject with a homozygous missense mutation in the AQP7 gene (28) that, on expression in *Xenopus laevis* oocytes, failed to show glycerol transport activity. However, the subject was not obese or diabetic. In the future, it will be interesting to examine if defects in AQP7 expression or regulation in β cells contribute to the development of type 2 diabetes.

ACKNOWLEDGMENTS

This work was supported in part by grants HL-51586, DK-68037 (both to L.C.), and RO1-DK67536 (to R.N.K.) from the U.S. National Institutes of Health and by a grant-in-aid (no. 18390100 to H. Kojima) for scientific research from the Ministry of Education, Culture, Sports, Science and Technology, Japan. This research was also supported in part by Public Health Service grant P30-DK56338, which funds the Texas Gulf Coast Digestive Diseases Center. W.C. and L.C. were supported by a mentor-based postdoctoral fellowship award from the American Diabetes Association (7-06-MN-10). L.C. was also supported in part by the Betty Rutherford Chair in Diabetes Research from St. Luke's Episcopal Hospital and Baylor College of Medicine, by the T. T. and W. F. Chao Global Foundation, by the Lydia and James Chao Fund, and by the Marcus Wray Fund.

REFERENCES

1. **Alcazar, O., E. Gine, Z. Qiu-Yue, and J. Tamarit-Rodriguez.** 1995. The stimulation of insulin secretion by D-glyceraldehyde correlates with its rate of oxidation in islet cells. Biochem. J. **310:**215–220.
2. **Ashcroft, S. J., L. C. Weerasinghe, and P. J. Randle.** 1973. Interrelationship of islet metabolism, adenosine triphosphate content and insulin release. Biochem. J. **132:**223–231.
3. **Borgnia, M., S. Nielsen, A. Engel, and P. Agre.** 1999. Cellular and molecular biology of the aquaporin water channels. Annu. Rev. Biochem. **68:**425–458.
4. **Calvo, E. L., N. J. Dusetti, M. B. Cadenas, J. C. Dagorn, and J. L. Iovanna.** 1991. Changes in gene expression during pancreatic regeneration: activation of c-myc and H-ras oncogenes in the rat pancreas. Pancreas **6:**150–156.
5. **Carbrey, J. M., D. A. Gorelick-Feldman, D. Kozono, J. Praetorius, S. Nielsen, and P. Agre.** 2003. Aquaglyceroporin AQP9: solute permeation and metabolic control of expression in liver. Proc. Natl. Acad. Sci. USA **100:** 2945–2950.
6. **Chang, B. H., W. Liao, L. Li, M. Nakamuta, D. Mack, and L. Chan.** 1999. Liver-specific inactivation of the abetalipoproteinemia gene completely abrogates very low density lipoprotein/low density lipoprotein production in a viable conditional knockout mouse. J. Biol. Chem. **274:**6051–6055.
7. **Demeterco, C., P. Itkin-Ansari, B. Tyrberg, L. P. Ford, R. A. Jarvis, and F. Levine.** 2002. c-Myc controls proliferation versus differentiation in human pancreatic endocrine cells. J. Clin. Endocrinol. Metab. **87:**3475–3485.
8. **Deng, S., M. Vatamaniuk, X. Huang, N. Doliba, M. M. Lian, A. Frank, E.**

Velidedeoglu, N. M. Desai, B. Koeberlein, B. Wolf, C. F. Barker, A. Naji, F. M. Matschinsky, and J. F. Markmann. 2004. Structural and functional abnormalities in the islets isolated from type 2 diabetic subjects. Diabetes **53:**624–632.

9. **Echevarria, M., E. E. Windhager, S. S. Tate, and G. Frindt.** 1994. Cloning and expression of AQP3, a water channel from the medullary collecting duct of rat kidney. Proc. Natl. Acad. Sci. USA **91:**10997–11001.
10. **Efrat, S., S. Linde, H. Kofod, D. Spector, M. Delannoy, S. Grant, D. Hanahan, and S. Baekkeskov.** 1988. Beta-cell lines derived from transgenic mice expressing a hybrid insulin gene-oncogene. Proc. Natl. Acad. Sci. USA **85:** 9037–9041.
11. **Engel, A., Y. Fujiyoshi, and P. Agre.** 2000. The importance of aquaporin water channel protein structures. EMBO J. **19:**800–806.
12. **Guan, H. P., Y. Li, M. V. Jensen, C. B. Newgard, C. M. Steppan, and M. A. Lazar.** 2002. A futile metabolic cycle activated in adipocytes by antidiabetic agents. Nat. Med. **8:**1122–1128.
13. **Hara-Chikuma, M., E. Sohara, T. Rai, M. Ikawa, M. Okabe, S. Sasaki, S. Uchida, and A. S. Verkman.** 2005. Progressive adipocyte hypertrophy in aquaporin-7-deficient mice: adipocyte glycerol permeability as a novel regulator of fat accumulation. J. Biol. Chem. **280:**15493–15496.
14. **Hashimoto, H., H. Ishikawa, and M. Kusakabe.** 1999. Preparation of whole mounts and thick sections for confocal microscopy. Methods Enzymol. **307:** 84–107.
15. **Hibuse, T., N. Maeda, T. Funahashi, K. Yamamoto, A. Nagasawa, W. Mizunoya, K. Kishida, K. Inoue, H. Kuriyama, T. Nakamura, T. Fushiki, S. Kihara, and I. Shimomura.** 2005. Aquaporin 7 deficiency is associated with development of obesity through activation of adipose glycerol kinase. Proc. Natl. Acad. Sci. USA **102:**10993–10998.
16. **Ishibashi, K., M. Kuwahara, Y. Gu, Y. Kageyama, A. Tohsaka, F. Suzuki, F. Marumo, and S. Sasaki.** 1997. Cloning and functional expression of a new water channel abundantly expressed in the testis permeable to water, glycerol, and urea. J. Biol. Chem. **272:**20782–20786.
17. **Ishibashi, K., T. Morinaga, M. Kuwahara, S. Sasaki, and M. Imai.** 2002. Cloning and identification of a new member of water channel (AQP10) as an aquaglyceroporin. Biochim. Biophys. Acta **1576:**335–340.
18. **Ishibashi, K., S. Sasaki, K. Fushimi, S. Uchida, M. Kuwahara, H. Saito, T. Furukawa, K. Nakajima, Y. Yamaguchi, and T. Gojobori.** 1994. Molecular cloning and expression of a member of the aquaporin family with permeability to glycerol and urea in addition to water expressed at the basolateral membrane of kidney collecting duct cells. Proc. Natl. Acad. Sci. USA **91:** 6269–6273.
19. **Johnson, J. D., N. T. Ahmed, D. S. Luciani, Z. Han, H. Tran, J. Fujita, S. Misler, H. Edlund, and K. S. Polonsky.** 2003. Increased islet apoptosis in Pdx1+/− mice. J. Clin. Investig. **111:**1147–1160.
20. **Jonas, J. C., A. Sharma, W. Hasenkamp, H. Ilkova, G. Patane, R. Laybutt, S. Bonner-Weir, and G. C. Weir.** 1999. Chronic hyperglycemia triggers loss of pancreatic beta cell differentiation in an animal model of diabetes. J. Biol. Chem. **274:**14112–14121.
21. **Kahn, S. E., D. K. McCulloh, and D. J. Porte.** 1997. Insulin secretion in the normal and diabetic human, p. 337–353. *In* K. G. M. M. Alberti, P. Zimmet, R. A. DeFronzo, and H. Keen (ed.), International textbook of diabetes mellitus. John Wiley & Sons, New York, NY.
22. **Kahn, S. E.** 2003. The relative contributions of insulin resistance and beta-cell dysfunction to the pathophysiology of type 2 diabetes. Diabetologia **46:**3–19.
23. **Kaneto, H., A. Sharma, K. Suzuma, D. R. Laybutt, G. Xu, S. Bonner-Weir, and G. C. Weir.** 2002. Induction of c-Myc expression suppresses insulin gene transcription by inhibiting NeuroD/BETA2-mediated transcriptional activation. J. Biol. Chem. **277:**12998–13006.
24. **Kaneto, H., K. Suzuma, A. Sharma, S. Bonner-Weir, G. L. King, and G. C. Weir.** 2002. Involvement of protein kinase C beta 2 in c-myc induction by high glucose in pancreatic beta-cells. J. Biol. Chem. **277:**3680–3685.
25. **Kishida, K., I. Shimomura, H. Kondo, H. Kuriyama, Y. Makino, H. Nishizawa, N. Maeda, M. Matsuda, N. Ouchi, S. Kihara, Y. Kurachi, T. Funahashi, and Y. Matsuzawa.** 2001. Genomic structure and insulin-mediated repression of the aquaporin adipose (AQPap), adipose-specific glycerol channel. J. Biol. Chem. **276:**36251–36260.
26. **Ko, S. B., S. Naruse, M. Kitagawa, H. Ishiguro, S. Furuya, N. Mizuno, Y. Wang, T. Yoshikawa, A. Suzuki, S. Shimano, and T. Hayakawa.** 2002. Aquaporins in rat pancreatic interlobular ducts. Am. J. Physiol. Gastrointest. Liver Physiol. **282:**G324–G331.
27. **Kojima, H., M. Fujimiya, K. Matsumura, T. Nakahara, M. Hara, and L. Chan.** 2004. Extrapancreatic insulin-producing cells in multiple organs in diabetes. Proc. Natl. Acad. Sci. USA **101:**2458–2463.
28. **Kondo, H., I. Shimomura, K. Kishida, H. Kuriyama, Y. Makino, H. Nishizawa, M. Matsuda, N. Maeda, H. Nagaretani, S. Kihara, Y. Kurachi, T. Nakamura, T. Funahashi, and Y. Matsuzawa.** 2002. Human aquaporin adipose (AQPap) gene. Genomic structure, promoter analysis and functional mutation. Eur. J. Biochem. **269:**1814–1826.
29. **Kulkarni, R. N., J. N. Winnay, M. Daniels, J. C. Bruning, S. N. Flier, D. Hanahan, and C. R. Kahn.** 1999. Altered function of insulin receptor substrate-1-deficient mouse islets and cultured beta-cell lines. J. Clin. Investig. **104:**R69–R75.
30. **Laybutt, D. R., G. C. Weir, H. Kaneto, J. Lebet, R. D. Palmiter, A. Sharma, and S. Bonner-Weir.** 2002. Overexpression of c-Myc in beta-cells of transgenic mice causes proliferation and apoptosis, downregulation of insulin gene expression, and diabetes. Diabetes **51:**1793–1804.
31. **Liu, Z., J. Shen, J. M. Carbrey, R. Mukhopadhyay, P. Agre, and B. P. Rosen.** 2002. Arsenite transport by mammalian aquaglyceroporins AQP7 and AQP9. Proc. Natl. Acad. Sci. USA **99:**6053–6058.
32. **MacDonald, M. J.** 2002. Differences between mouse and rat pancreatic islets: succinate responsiveness, malic enzyme, and anaplerosis. Am. J. Physiol. Endocrinol. Metab. **283:**E302–E310.
33. **Maeda, N., T. Funahashi, T. Hibuse, A. Nagasawa, K. Kishida, H. Kuriyama, T. Nakamura, S. Kihara, I. Shimomura, and Y. Matsuzawa.** 2004. Adaptation to fasting by glycerol transport through aquaporin 7 in adipose tissue. Proc. Natl. Acad. Sci. USA **101:**17801–17806.
34. **Mobasheri, A., M. Shakibaei, and D. Marples.** 2004. Immunohistochemical localization of aquaporin 10 in the apical membranes of the human ileum: a potential pathway for luminal water and small solute absorption. Histochem. Cell Biol. **121:**463–471.
35. **Morinaga, T., M. Nakakoshi, A. Hirao, M. Imai, and K. Ishibashi.** 2002. Mouse aquaporin 10 gene (AQP10) is a pseudogene. Biochem. Biophys. Res. Commun. **294:**630–634.
36. **Nagy, A., E. Gocza, E. M. Diaz, V. R. Prideaux, E. Ivanyi, M. Markkula, and J. Rossant.** 1990. Embryonic stem cells alone are able to support fetal development in the mouse. Development **110:**815–821.

36a. **NIH.** 1985. Principles of laboratory animal care. Publication no. 85023. NIH, Bethesda, MD.

37. **Noel, R. J., P. A. Antinozzi, J. D. McGarry, and C. B. Newgard.** 1997. Engineering of glycerol-stimulated insulin secretion in islet beta cells. Differential metabolic fates of glucose and glycerol provide insight into mechanisms of stimulus-secretion coupling. J. Biol. Chem. **272:**18621–18627.
38. **Prudente, S., E. Flex, E. Morini, F. Turchi, D. Capponi, S. De Cosmo, V. Tassi, V. Guida, A. Avogaro, F. Folli, F. Maiani, L. Frittitta, B. Dallapiccola, and V. Trischitta.** 2007. A functional variant of the adipocyte glycerol channel aquaporin 7 gene is associated with obesity and related metabolic abnormalities. Diabetes **56:**1468–1474.
39. **Skelly, R. H., B. Wicksteed, P. A. Antinozzi, and C. J. Rhodes.** 2001. Glycerol-stimulated proinsulin biosynthesis in isolated pancreatic rat islets via adenoviral-induced expression of glycerol kinase is mediated via mitochondrial metabolism. Diabetes **50:**1791–1798.
40. **Skowronski, M. T., J. Lebeck, A. Rojek, J. Praetorius, E. M. Fuchtbauer, J. Frokiaer, and S. Nielsen.** 2007. AQP7 is localized in capillaries of adipose tissue, cardiac and striated muscle: implications in glycerol metabolism. Am. J. Physiol. Renal Physiol. **292:**F956–F965.
41. **Tsukaguchi, H., C. Shayakul, U. V. Berger, B. Mackenzie, S. Devidas, W. B. Guggino, A. N. van Hoek, and M. A. Hediger.** 1998. Molecular characterization of a broad selectivity neutral solute channel. J. Biol. Chem. **273:**24737–24743.
42. **Weir, G. C., D. R. Laybutt, H. Kaneto, S. Bonner-Weir, and A. Sharma.** 2001. Beta-cell adaptation and decompensation during the progression of diabetes. Diabetes **50**(Suppl. 1)**:**S154–S159.
43. **Zawalich, W. S., K. C. Zawalich, G. J. Tesz, J. A. Sterpka, and W. M. Philbrick.** 2001. Insulin secretion and IP levels in two distant lineages of the genus Mus: comparisons with rat islets. Am. J. Physiol. Endocrinol. Metab. **280:**E720–E728.